Scattering Function of Oligo- and Poly(α-methylstyrene)s in Dilute Solution

Yoshimi Ohgaru, Masakazu Sumida, Masashi Osa,† Takenao Yoshizaki, and Hiromi Yamakawa*

Department of Polymer Chemistry, Kyoto University, Kyoto 606-8501, Japan

Received July 5, 2000; Revised Manuscript Received September 25, 2000

ABSTRACT: The scattering function was determined for four samples of atactic oligo- and poly(α-methylstyrene)s (a-PαMS), each with the fraction of racemic diads $f_r = 0.72$, in the range of weight-average molecular weight M_w from 1.27×10^3 to 6.46×10^4 in cyclohexane at 30.5 °C (Θ) in the range of the magnitude k of the scattering vector smaller than 1 Å^{-1} by the use of a point-focusing small-angle X-ray scattering (SAXS) camera. The Kratky function F_s as a function of k increases monotonically with increasing k for $M_w \lesssim 5 \times 10^3$ and exhibits a plateau in the range of 0.15 Å$^{-1} \lesssim k \lesssim 0.3$ Å^{-1} for $M_w \gtrsim 5 \times 10^3$. For $k \lesssim 0.5$ Å^{-1}, all the experimental data may be well explained by the corresponding helical wormlike (HW) chain theory. For $k \gtrsim 0.5$ Å^{-1}, however, agreement between theory and experiment is only qualitative. A comparison is made of the present SAXS data for a-PαMS with the previous data for atactic polystyrene with $f_r = 0.59$, atactic poly(methyl methacrylate) (a-PMMA) with $f_r = 0.79$, isotactic PMMA with $f_r \simeq 0.01$, and syndiotactic (s-) PMMA with $f_r = 0.92$. It is then found that the HW theory may give a good explanation of the difference in the behavior of F_s for $k \lesssim 0.3$ Å^{-1} between the four polymers except s-PMMA, for which the HW model parameters have not been determined.

Introduction

In a previous paper,[1] we made a start in the study of dilute solution properties of atactic oligo- and poly(α-methylstyrene)s (a-PαMS) with the fraction of racemic diads $f_r = 0.72$ on the basis of the helical wormlike (HW) chain model[2,3] by determining the mean-square radius of gyration $\langle S^2 \rangle$ in the unperturbed state (in cyclohexane at Θ). It was found that the plot of the ratio $\langle S^2 \rangle$ to the degree of polymerization x as a function of x first increases steeply for $x \lesssim 20$, then passes through a flat hump at $x \simeq 40$, and finally approaches its asymptotic value for $x \gtrsim 1 \times 10^3$, and from an analysis of the plot of those data, the HW model parameters for the a-PαMS chain were unambiguously determined. It was then shown from those parameter values that the chain is rather stiff (its static stiffness parameter λ^{-1} being 46.8 Å) and tends to retain large and clearly distinguishable helical portions in dilute solution (having a rather strong helical nature), as was expected from the chemical structure of a-PαMS. Further, a comparison was made of the results for a-PαMS with the previous ones for atactic polystyrene (a-PS) with $f_r = 0.59$,[2−5] atactic poly(methyl methacrylate) (a-PMMA) with $f_r = 0.79$,[2,3,6,7] and isotactic (i-) PMMA with $f_r \simeq 0.01$,[2,3,8] leading to the conclusion that the order of the magnitude of λ^{-1} and also of the strength of helical nature is a-PMMA > a-PαMS > i-PMMA > a-PS. Such differences in chain stiffness and local chain conformation may be expected to be more clearly reflected in the behavior of the scattering function P_s determined from small-angle X-ray scattering (SAXS) measurements. Thus, in this paper, we proceed to study P_s of a-PαMS (in cyclohexane at Θ) and compare the results with the previous ones for a-PS,[9] a- and i-PMMAs[10,11] and also syndiotactic (s-) PMMA with $f_r = 0.92$.[12]

† Research Fellow of the Japan Society for the Promotion of Science.

In the previous studies[9−12] of P_s mentioned above, it was found that for a- and s-PMMAs the Kratky plot of Mk^2P_s against the magnitude k of the scattering vector exhibits a maximum followed by a minimum in the range of $k \lesssim 0.3$ Å^{-1} for the molecular weight $M \gtrsim 5 \times 10^3$. This feature of the plot is characteristic of a polymer chain of strong helical nature, and therefore this is not the case with a-PS and i-PMMA. These results are consistent with the corresponding HW theory,[2,3,13,14] which predicts the dependence of the behavior of the plot on chain stiffness and local chain conformation in such a range of small k. The main purpose of this paper is therefore to examine whether or not the behavior of the plot for a-PαMS may also be consistently explained by the HW theory using the values of the model parameters determined in the previous paper[1] on $\langle S^2 \rangle$.

The present SAXS measurements for a-PαMS were carried out by the use of the same point-focusing camera as that in the previous studies for a-PS[9] and the three kinds of PMMAs.[10−12] This camera has the advantage of enabling us to determine P_s directly without the use of the desmearing procedure. We note that SAXS measurements by the use of a Kratky camera with the desmearing procedure inherent in it reduce the reliability of the data in the range of large k ($\gtrsim$0.4 Å^{-1}), as previously noted.[10−12]

Experimental Section

Materials. The four a-PαMS samples used in this work are the same as those used in the previous study of $\langle S^2 \rangle$,[1] i.e., fractions separated by gel permeation chromatography (GPC) and/or fractional precipitation from the original samples prepared by living anionic polymerization. The values of f_r for these samples are 0.72, independent of the weight-average molecular weight M_w.[15] The values of M_w determined from light scattering (LS) measurements in cyclohexane at 30.5 °C (Θ),[1] the weight-average degree of polymerization x_w calculated from M_w, the ratio of M_w to the number-average molecular weight

10.1021/ma0011542 CCC: $19.00
Published on Web 11/16/2000

Table 1. Values of M_w, x_w, M_w/M_n, and $\langle S^2\rangle^{1/2}$ for Atactic Oligo- and Poly(α-methylstyrene)s

sample	M_w	x_w	M_w/M_n	$\langle S^2\rangle^{1/2}$, Å
OAMS10[a]	1.27×10^3	10.3	1.01	7.5_6
OAMS25	2.96×10^3	24.6	1.06	$13._8$
OAM67	7.97×10^3	67.1	1.04	$23._4$
AMS6	6.46×10^4	547	1.03	$66._7$

[a] All values of M_w had been determined from LS in cyclohexane at 30.5 °C,[1] and all values $\langle S^2\rangle^{1/2}$ from SAXS also in cyclohexane at 30.5 °C.[1]

M_n determined by analytical GPC,[1] and the root-mean-square radius of gyration $\langle S^2\rangle^{1/2}$ determined from SAXS measurements in cyclohexane at Θ by the use of a Kratky camera[1] are summarized in Table 1.

The solvent cyclohexane used for SAXS measurements was purified according to a standard procedure.

Small-Angle X-ray Scattering. As in the previous SAXS studies,[9−12] all measurements were carried out by the use of a point-focusing camera of overall length 6 m in the High-Intensity X-ray Laboratory of Kyoto University. A detailed specification of this camera has already been given elsewhere[16] and its brief description has been given in the previous paper.[9] Thus we note here only a few points appropriate to the present work.

In this work, the Mo Kα line of wavelength $\lambda_0 = 0.711$ Å was used as the incident beam by eliminating other lines with a Zr foil of 50-μm thickness. The distance from a sample cell to a detector (two-dimensional position-sensitive proportional counter) was ca. 640 mm as before,[9−12] so that intensity measurements could be carried out in the range of k up to ca. 1 Å^{-1}. The temperature of the sample cell was kept constant at 30.5 ± 0.1 °C for the cyclohexane solutions. The excess scattered intensity in the range of $k \gtrsim 0.5$ Å^{-1} was very small. Therefore, in order to diminish statistical errors in this range, the intensities scattered from each solution and the solvent were accumulated for ca. 12 and 6 h, respectively. The measurements for the solvent were made before and after every measurement for the solution.

As in the previous studies,[9−12] the two-dimensional data so obtained for a solution of solute mass concentration c (in g/cm^3) were first corrected for the detector sensitivity, and then they were averaged over polar angles in the detector plane to obtain the scattered intensity $I_{obs}(k,c)$ as a function of k, which is explicitly defined by

$$k = (4\pi/\lambda_0)\sin(\theta/2) \tag{1}$$

with θ the scattering angle. From the observed intensity I_{obs}, we calculate the reduced intensity $I_R(k,c)$ defined by

$$I_R(k,c) = I_{obs}(k,c)/AI_0 \tag{2}$$

where A is the transmittance of a given sample solution and I_0 is the intensity of the incident beam monitored by the intensity scattered from a polyethylene film placed in front of the detector. The excess reduced intensity $\Delta I_R(k,c)$ is then obtained as the reduced intensity from the solution $I_{R,soln}(k,c)$ minus that from the solvent $I_{R,solv}(k)$ [$= I_{R,soln}(k,0)$] as follows

$$\Delta I_R(k,c) = I_{R,soln}(k,c) - I_{R,solv}(k) \tag{3}$$

Results

Following the same procedure as that used in the previous studies[9−11] of the scattering function, we first evaluate the (normalized) scattering function P_s from the values of the excess reduced intensity $\Delta I_R(k,c)$, which are directly obtained from SAXS measurements, as mentioned in the Experimental Section.

It may be summarized as follows. The quantity $\Delta I_R(k,c)$ may be written in terms of P_s as[9−11]

$$\frac{Kc}{\Delta I_R(k,c)} = \frac{1}{M_w P_s(k)} + 2A_2Q(k)\,c + O(c^2) \tag{4}$$

where K is the optical constant, A_2 is the second virial coefficient, and Q represents the intermolecular interference.[17] (Note that P_s and Q become unity at $k = 0$.) From eq 4, we obtain

$$\frac{\Delta I_R(k,c)}{KM_w c} = P_s(k) - 2A_2M_w[P_s(k)]^2Q(k)\,c + O(c^2) \tag{5}$$

We may then evaluate P_s by extrapolating the ratio $\Delta I_R(k,c)/KM_wc$ to $c = 0$ if the value of K is known. In the limits of $k \to 0$ and $c \to 0$, we have from eq 4

$$K = [\Delta I_R(0,c)/c]_{c=0}/M_w \tag{6}$$

Thus K may be evaluated experimentally if the value of $[\Delta I_R(0,c)/c]_{c=0}$ is determined for a sample whose M_w is known.

In the present case, we evaluated $[\Delta I_R(0,c)/c]_{c=0}$ for the sample OAMS25 in cyclohexane at 30.5 °C by the use of the Berry square-root plot.[18] For each solution of this sample, the plot of $(c/\Delta I_R)^{1/2}$ against k^2 followed a straight line in the range of small k, so that the intercept $[c/\Delta I_R(0,c)]^{1/2}$ at a given c could be unambiguously determined. Similarly, in the range of small k, the plot of $(c/\Delta I_R)^{1/2}$ against c was fitted by a straight line and could be extrapolated to infinite dilution to evaluate $[c/\Delta I_R(k,c)]_{c=0}{}^{1/2}$ at a given (small) k. The values of $[c/\Delta I_R(0,c)]^{1/2}$ and $[c/\Delta I_R(k,c)]_{c=0}{}^{1/2}$ so determined for the sample OAMS25 are plotted against c and k^2, respectively, in Figure 1. The two kinds of plots can be extrapolated to obtain the common intercept $[c/\Delta I_R(0,c)]_{c=0}{}^{1/2} = 78.2$ (g/cm^3)$^{1/2}$. With the value of M_w for the sample OAMS25 given in Table 1, K is thus evaluated to be 5.52×10^{-8} cm^3/g. It is seen from the figure that A_2 is definitely positive for this sample in cyclohexane at Θ. This is consistent with the previous result[1] that A_2 is positive for a-PαMS oligomers.

Before presenting results for the scattering function, it is interesting to compare here the value of the apparent mean-square radius of gyration $\langle S^2\rangle_s$, which may be obtained from the data given in Figure 1, with that determined in the previous paper[1] on $\langle S^2\rangle$. Recall that $\langle S^2\rangle_s$ is defined in the equation

$$P_s(k) = 1 - (^1/_3)\langle S^2\rangle_s\,k^2 + O(k^4) \tag{7}$$

It may then be determined from the intercept and initial slope of the plot of $[c/\Delta I_R(k,c)]_{c=0}{}^{1/2}$ against k^2 in Figure 1. The result so obtained for $\langle S^2\rangle_s$ is 191 Å^2. This value is in rather good agreement with the corresponding value 201 Å^2 previously determined,[1] indicating that the present determination of the scattered intensity is consistent with the previous one with a Kratky camera in the range of small k. (Note that $\langle S^2\rangle_s$ should in general be distinguished from the mean-square radius of gyration $\langle S^2\rangle$ of the chain contour except for long enough chains.[1,2])

Now, $k^2\Delta I_R(k,c)/Kc$ are plotted against k in Figure 2 for the sample OAMS25 in cyclohexane at various c at 30.5 °C. The ordinate quantity corresponds to the (absolute-scale) Kratky function $F_s(k)$ defined by

$$F_s(k) = M_w\,k^2P_s(k) \tag{8}$$

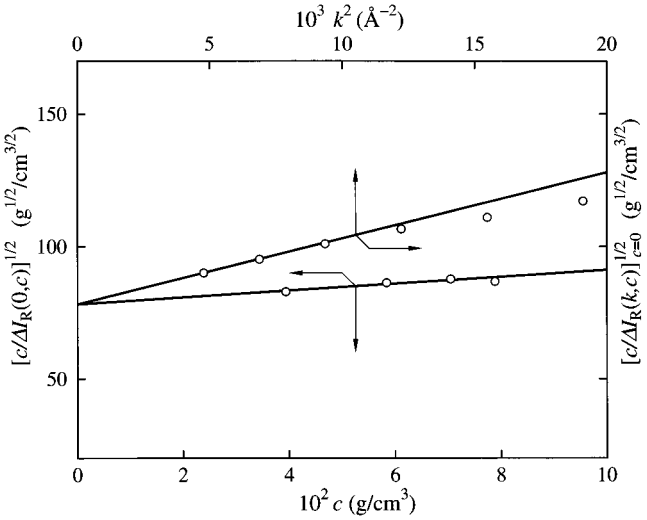

Figure 1. Plots of $[c/\Delta I_R(0,c)]^{1/2}$ and $[c/\Delta I_R(k,c)]_{c=0}^{1/2}$ against c and k^2, respectively, for sample OAMS25 in cyclohexane at 30.5 °C.

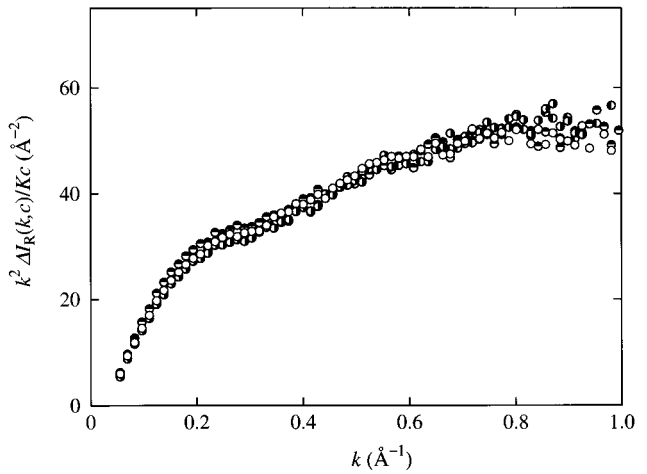

Figure 2. Plots of $k^2\Delta I_R(k,c)/Kc$ against k for sample OAMS25 in cyclohexane at 30.5 °C: (○) $c = 0.0788$ g/cm^3; (◑) $c = 0.0704$ g/cm^3; (◐) $c = 0.0584$ g/cm^3; (◓) $c = 0.0394$ g/cm^3.

(at finite concentrations), the above plot being just the Kratky plot. In the figure, the unfilled, right-half-filled, left-half-filled, and top-half-filled circles represent the values at $c = 0.0788$, 0.0704, 0.0584, and 0.0394 g/cm^3, respectively. It is seen that the plot is almost independent of c in the range of k displayed, as in the cases of a-, i-, and s-PMMAs,[10−12] so that we adopt as before[10−12] the values of $\Delta I_R(k,c)/KM_wc$ at the highest concentration as those of the scattering function P_s for the single polymer chain at infinite dilution. We note that in the range of small k, the concentration dependence is appreciable ($A_2 > 0$, as mentioned above) in the plot displayed in Figure 1 but cannot be recognized in the Kratky plot.

Figure 3 shows plots of $F_s(k)$ against k for all the a-PαMS samples in cyclohexane at 30.5 °C, where the data points for the samples OAMS25, OAMS67, and AMS6 have been shifted upward by 40, 80, and 120 Å^{-2}, respectively, for convenience. It also includes the previous data[1] obtained for the same samples (small circles) by the use of a Kratky camera in the range of $k \lesssim 0.05$ Å^{-1}, where F_s could not be obtained under the setting condition of the (point-focusing) SAXS camera for the present purpose. The plot increases monotonically with increasing k for the samples OAMS10 and OAMS25. On the other hand, it exhibits a plateau in the range of 0.15 Å$^{-1} \lesssim k \lesssim 0.3$ Å^{-1} for the sample OAMS67 and in the range of 0.1 Å$^{-1} \lesssim k \lesssim 0.3$ Å^{-1} for the sample AMS6. In the figure the curves represent the HW theoretical values, which are discussed in the next section.

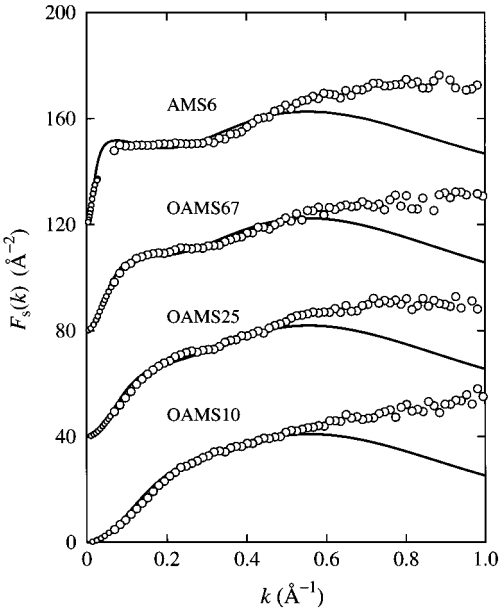

Figure 3. Plots of $F_s(k)$ against k for all the samples: (○) data in cyclohexane at 30.5 °C; (solid curves) best-fit HW theoretical values. The large and small circles represent the present and previous[1] data, respectively. The data points and the theoretical curves for samples OAMS25, OAMS67, and AMS6 are shifted upward by 40, 80, and 120 Å^{-2}, respectively.

Discussion

Kratky Function. Figure 4 shows plots of F_s against k for all the a-PαMS samples in cyclohexane at 30.5 °C, which have been reproduced from Figure 3. The unfilled, right-half-filled, left-half-filled, and top-half-filled circles represent the values for the samples OAMS10, OAMS25, OAMS67, and AMS6, respectively, the large and small circles representing the present and previous[1] data, respectively. It is seen that the present data points may be smoothly joined to the previous ones for all the samples except for AMS6, for which the two kinds of data points do not overlap with each other. This continuity between them confirms the appropriateness and accuracy of the present determination of F_s described in the Results. In Figure 4 the solid curve connects smoothly the two kinds of data points for each sample.

As in the cases of a- and i-PMMAs previously studied,[10,11] the behavior of F_s depends clearly on M_w in the range of $k \lesssim 0.3$ Å^{-1} but is rather insensitive to change in M_w in the range of $k \gtrsim 0.4$ Å^{-1}. This implies that the electronic environment around the a-PαMS chain, which is reflected in the behavior of F_s in the latter range of k, is independent of M_w. For all the samples, F_s does not exhibit a maximum (followed by a minimum) such as observed for a- and s-PMMAs with large M_w.[10,12] This indicates that the a-PαMS chain is of weaker helical nature than the a- and s-PMMA chains, the result being consistent with the previous one of an analysis of $\langle S^2 \rangle$.[1]

Comparison with the HW Theory. Now we make a comparison of the present and previous[1] experimental data for F_s with the corresponding HW theory,[2,13,14] in which the effect of chain thickness [i.e., thickness of the

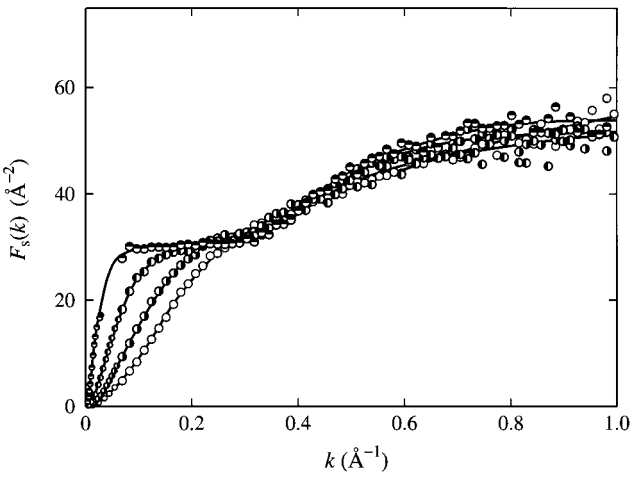

Figure 4. Plots of $F_s(k)$ against k for all the samples in cyclohexane at 30.5 °C: (○) OAMS10; (◑) OAMS25; (◐) OAMS67; (◓) AMS6. The large and small circles represent the present and previous[1] data, respectively. The solid curve connects smoothly the data points for each sample.

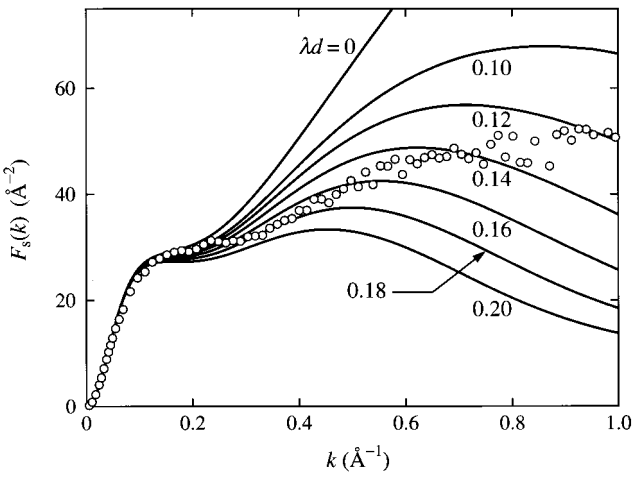

Figure 5. Comparison of the observed values of F_s for sample OAMS67 with the HW theoretical values: (○) data in cyclohexane at 30.5 °C; (solid curves) HW theoretical values for the indicated values of λd.

spatial distribution of (excess) electrons (scatterers) around the HW chain contour] has been taken into account by adopting two simple models: the cylinder model and the touched-spheroid model. As in the case of the previous analysis of the SAXS data for a-PS[9] and a- and i-PMMAs,[10,11] we consider here only the former model, for simplicity.

For the HW cylinder model of total contour length L and diameter d, the scattering function $P_s(k;L)$ is given by eq 5.49 (with eq 5.56) of ref 2, which may be written in terms of the characteristic function I (i.e., the Fourier transform of the distribution function of the end-to-end vector distance), the angular correlation function[2,19] $g_l^{jj'}$ with $l = 2$ and $j = j' = 0$ given by eq 5.57 of ref 2, and the functions F_n ($n = 0$, 1) of kd given by eqs 5.58 and 5.59 of ref 2. The functions I and g_2^{00} depend on the three basic model parameters of the HW chain, i.e., the constant differential-geometrical curvature κ_0 and torsion τ_0 of its characteristic helix taken at the minimum zero of its elastic energy and the static stiffness parameter λ^{-1}, while the functions F_n are independent of them. [The functions F_n represent the effects of the (uniform) spatial distribution of electrons within the (flexible) cylinder.] We note that the function I may be evaluated numerically by the use of the weighting function and ϵ methods,[2,20] so that $P_s(k;L)$ may also be evaluated numerically for given k and L. We also note that for the HW chain with finite diameter F_s vanishes in the limit of $k \to \infty$, since P_s is proportional to k^{-4} in this limit. In order to compare the theoretical values of P_s as a function of k for given values of L and d with the experimental values, L may be converted to M_w by the use of the relation

$$L = M_w/M_L \tag{9}$$

with M_L the shift factor defined as the molecular weight per unit contour length. The Kratky function F_s may then be calculated theoretically from eq 8 with the values of P_s so obtained numerically and with eq 9.

In the previous cases of the a-PS[9] and i-PMMA[11] chains of weak helical nature, the experimental data for F_s in the range of $k \lesssim 0.25$ Å^{-1} have been well reproduced by the theory using the values of the HW model parameters determined from $\langle S^2 \rangle$ along with that of d properly assigned. On the other hand, in the case of the a-PMMA chain[10] of strong helical nature, agreement between theory and experiment is not satisfactory even in such a range of small k where the effect of d may be neglected, if the values of λ^{-1} and M_L determined from $\langle S^2 \rangle$ are used as they stand. These values were therefore slightly changed so that the theory agreed well with the experimental results for a-PMMA. The situation for the a-PαMS chain of rather strong helical nature is similar to that for a-PMMA. Thus we have changed the values of λ^{-1} and M_L from 46.8 Å and 39.8 Å^{-1} previously[1] determined from $\langle S^2 \rangle$ to 40.2 Å and 41.0 Å^{-1}, respectively, so that the theory agrees well with the experimental results for all the a-PαMS samples in such a small range of k. We note that such small changes in λ^{-1} and M_L do not affect the order of the magnitude of λ^{-1} and of the strength of helical nature (for the four polymers) mentioned in the Introduction.

Figure 5 shows plots of F_s against k for the a-PαMS sample OAMS67 in cyclohexane at 30.5 °C. The unfilled circles represent the (present and previous) experimental values, and the solid curves represent the corresponding HW theoretical values calculated from eq 8 with eq 9 with the values of the model parameters mentioned above and those of λd indicated. It is seen that in the range of $k \lesssim 0.1$ Å^{-1}, the theoretical values are in rather good agreement with the experimental ones irrespective of the values of λd. For larger k, however, the theory cannot give a quantitative explanation of the experimental results. Thus a theoretical curve such that in the range of $k \lesssim 0.5$ Å^{-1} it is close to the experimental data is adopted as the "best-fit" theoretical curve, for convenience. In this case, the curve with $\lambda d = 0.16$ is such a best-fit one.

In Figure 3, the "best-fit" HW theoretical values calculated for all the a-PαMS samples from eq 8 with eq 9 with the values of the model parameters mentioned above and with $\lambda d = 0.16$ are also represented by the solid curves. For the samples OAMS25, OAMS67, and AMS6, they have also been shifted upward by 40, 80, and 120 Å^{-2}, respectively. It is seen that the theory may explain rather well the experimental data in the range of $k \lesssim 0.5$ Å^{-1} but fails to reproduce quantitatively the behavior of F_s in the range of large $k \gtrsim 0.5$ Å^{-1} since it takes no account of the detailed spatial distribution of electrons. It is interesting to estimate here the value of

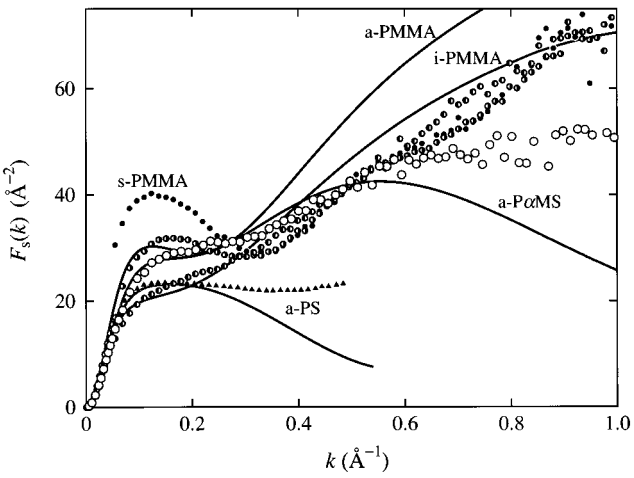

Figure 6. Comparison of the data for a-PαMS with those for a-PS and a-, i-, and s-PMMAs: (○) present data for sample OAMS67 in cyclohexane at 30.5 °C; (▲) previous data for an a-PS sample with $M_w = 1.01 \times 10^4$ in cyclohexane at 34.5 °C;[9] (◑) previous data for an a-PMMA sample with $M_w = 1.09 \times 10^4$ in acetonitrile at 44.0 °C;[10] (◐) previous data for an i-PMMA sample with $M_w = 1.01 \times 10^4$ in acetonitrile at 28.0 °C;[11] (●) previous data for an s-PMMA sample with $M_w = 3.76 \times 10^4$ in acetonitrile at 44.0 °C;[12] (solid curves) best-fit HW theoretical values for all the samples except for the s-PMMA one.

the diameter d of this distribution. We have $d = 6.4$ Å from the above values of λd and λ^{-1}. This value of d is somewhat smaller than the value 9.2 Å previously[1] estimated from the partial specific volume. The present value 6.4 Å of d for a-PαMS is larger than the values 2.8 Å for a-PMMA[10] and 3.0 Å for i-PMMA,[11] indicating that the thickness of the spatial distribution of electrons around the chain contour is larger for PαMS with the phenyl group than for PMMA with the ester group.

Comparison with the Other Polymers. Finally, we make a comparison of the present (and previous) SAXS data for F_s for a-PαMS with the previous ones for a-PS[9] and a-, i- and s-PMMAs.[10−12] This is shown in Figure 6, where the unfilled circles represent the data for the a-PαMS sample OAMS67 (with $f_r = 0.72$ and $M_w = 7.97 \times 10^3$) in cyclohexane at 30.5 °C, the filled triangles for an a-PS sample with $f_r = 0.59$ and $M_w = 1.01 \times 10^4$ in cyclohexane at 34.5 °C,[9] the right-half-filled circles for an a-PMMA sample with $f_r = 0.79$ and $M_w = 1.09 \times 10^4$ in acetonitrile at 44.0 °C,[10] the left-half-filled circles for an i-PMMA sample with $f_r \simeq 0.01$ and $M_w = 1.01 \times 10^4$ in acetonitrile at 28.0 °C,[11] and the filled circles for an s-PMMA sample with $f_r = 0.92$ and $M_w = 3.76 \times 10^4$ in acetonitrile at 44.0 °C.[12] The solid curves represent the best-fit HW theoretical values for the respective polymer samples except for the s-PMMA one, for which the HW model parameters have not been determined. The theoretical values have been calculated from eq 8 with eq 9 with the values of the model parameters ($\lambda^{-1}\kappa_0$, $\lambda^{-1}\tau_0$, λ^{-1}/Å, M_L/Å^{-1}, λd) equal to (3.0, 6.0, 22.5, 36.7, 0.61) for a-PS,[9] (4.0, 1.1, 47.0, 38.0, 0.06) for a-PMMA,[10] and (2.5, 1.3, 38.0, 32.5, 0.08) for i-PMMA.[11]

It is clearly seen from Figure 6 that, in the range of $k \lesssim 0.3$ Å^{-1}, the difference in the behavior of F_s between the four polymers except s-PMMA may be well explained by the HW theory using the above values of the model parameters (consistent with those from $\langle S^2 \rangle$). The indication is that the HW chain model may give a good explanation of dilute solution behavior of polymers, especially in the range where the significant effects of chain stiffness and local chain conformations appear. We note that although M_w of the s-PMMA sample is somewhat larger than those of the other polymer samples (with $M_w \simeq 10^4$), the theory[13] predicts that such an increase in M_w causes only a small shift of the maximum in F_s to the left. It is then seen from the behavior of F_s that the s-PMMA chain is of the strongest helical nature of all the above five polymers, although its model parameters have not been determined. As for the shape of the curve of F_s in the range of small k, we must re-emphasize that the observed height of the so-called plateau in F_s is equal to $2M_w/\langle S^2 \rangle$ for the Gaussian chain, while the HW chain theory predicts that this is not true.[2]

However, the HW theory may give only a qualitative explanation of the behavior of F_s in the range of $k \gtrsim 0.4$ Å^{-1}, since the details of the spatial distribution of electrons around the chain contour have not been taken into account. Further, it is important to note that both experimentally and theoretically, a second maximum followed by a second minimum (oscillation) in F_s cannot be observed, although the rotational isomeric state (RIS) model[21] predicts such oscillation for s-PMMA[22] (and also for a-PMMA with large f_r[14]). The oscillation indicates the "crystal-like" behavior of the chain, and its occurrence should rather be regarded as a defect of the RIS model.[2]

Conclusion

The scattering function P_s, or the Kratky function F_s, has been determined accurately for the four a-PαMS samples with different M_w, including the oligomers, each with the fraction of racemic diads $f_r = 0.72$, in the unperturbed Θ state in the range of the scattering vector $k < 1$ Å^{-1} by the use of a point-focusing SAXS camera in the High-Intensity X-ray Laboratory of Kyoto University. It is found that F_s as a function of k increases monotonically with increasing k for $M_w \lesssim 5 \times 10^3$ and exhibits a plateau in the range of 0.15 Å$^{-1} \lesssim k \lesssim 0.3$ Å^{-1} for $M_w \gtrsim 5 \times 10^3$. From a comparison of the experimental data with the corresponding HW theory, it is found that agreement between theory and experiment is satisfactory in the range of $k \lesssim 0.5$ Å^{-1} but is only qualitative in the range of $k \gtrsim 0.5$ Å^{-1}. A comparison is also made of the present data with the previous ones for a-PS[9] and a-, i-, and s-PMMAs.[10−12] The behavior of F_s is found to depend appreciably on the kind of polymer in the range of $k \lesssim 0.3$ Å^{-1}. This difference in the behavior of F_s may be well explained by the HW theory which can describe the effects of chain stiffness and local chain conformations. In the following paper,[23] we study the intrinsic viscosity $[\eta]$ and translational diffusion coefficient D.

References and Notes

(1) Osa, M.; Yoshizaki, T.; Yamakawa, H. *Macromolecules* **2000**, *33*, 4828.
(2) Yamakawa, H. *Helical Wormlike Chains in Polymer Solutions*; Springer: Berlin, 1997.
(3) Yamakawa, H. *Polym. J.* **1999**, *31*, 109.
(4) Konishi, T.; Yoshizaki, T.; Saito, T.; Einaga, Y.; Yamakawa, H. *Macromolecules* **1990**, *23*, 290.
(5) Abe, F.; Einaga, Y.; Yoshizaki, T.; Yamakawa, H. *Macromolecules* **1993**, *26*, 1884.
(6) Tamai, Y.; Konishi, T.; Einaga, Y.; Fujii, M.; Yamakawa, H. *Macromolecules* **1990**, *23*, 4067.
(7) Abe, F.; Horita, K.; Einaga, Y.; Yamakawa, H. *Macromolecules* **1994**, *27*, 725.

(8) Kamijo, M.; Sawatari, N.; Konishi, T.; Yoshizaki, T.; Yamakawa, H. *Macromolecules* **1994**, *27*, 5697.
(9) Koyama, H.; Yoshizaki, T.; Einaga, Y.; Hayashi, H.; Yamakawa, H. *Macromolecules* **1991**, *24*, 932.
(10) Yoshizaki, T.; Hayashi, H.; Yamakawa, H. *Macromolecules* **1993**, *26*, 4037.
(11) Horita, K.; Yoshizaki, T.; Hayashi, H.; Yamakawa, H. *Macromolecules* **1994**, *27*, 6492.
(12) Yoshizaki, T.; Hayashi, H.; Yamakawa, H. *Macromolecules* **1994**, *27*, 4259.
(13) Yoshizaki, T.; Yamakawa, H. *Macromolecules* **1980**, *13*, 1518.
(14) Nagasaka, K.; Yoshizaki, T.; Shimada, J.; Yamakawa, H. *Macromolecules* **1991**, *24*, 924.
(15) Osa, M.; Sumida, M.; Yoshizaki, T.; Yamakawa, H.; Ute, K.; Kitayama, T.; Hatada, K. *Polym. J.* **2000**, *32*, 361.
(16) Hayashi, H.; Hamada, F.; Suehiro, S.; Masaki, N.; Ogawa, T.; Miyaji, H. *J. Appl. Crystallogr.* **1988**, *21*, 330.
(17) Yamakawa, H. *Modern Theory of Polymer Solutions*; Harper & Row: New York, 1971.
(18) Berry, G. C. *J. Chem. Phys.* **1966**, *44*, 4550.
(19) Yamakawa, H.; Shimada, J. *J. Chem. Phys.* **1979**, *70*, 609.
(20) Yamakawa, H.; Shimada, J.; Fujii, M. *J. Chem. Phys.* **1978**, *68*, 2140.
(21) Flory, P. J. *Statistical Mechanics of Chain Molecules*; Interscience: New York, 1969.
(22) Yoon, D. Y.; Flory, P. J. *Macromolecules* **1976**, *9*, 299.
(23) Suda, I.; Tominaga, Y.; Osa, M.; Yoshizaki, T.; Yamakawa, H. *Macromolecules* **2000**, *33*, 9322.

MA0011542